

---

# Spatiotemporal Neural Activities Involved in the Olfactory Processing of the Land Slug using Fluorescent-Imaging Technique

---

Minoru Saito

Additional information is available at the end of the chapter

<http://dx.doi.org/10.5772/intechopen.69459>

---

## Abstract

The brain or central nervous system forms a network composed of so many neurons and their function is based on complex interactions among electric neural activities, intracellular calcium signals, intercellular communications by neurotransmitter, and so on. For multi-point measurement of neural activities, fluorescent-imaging technique using voltage-sensitive dyes or calcium-sensitive dyes can be a powerful technique. This technique has been applied to measure spatiotemporal neural activities involved in the olfactory processing of the land slug *Limax*. In *Limax*, the procerebral (PC) lobe, which is the olfactory center located in the lateral part of each cerebral ganglion, spontaneously produces a periodic oscillation of local field potential (LFP) of about 1 Hz, and the phase of the LFP oscillation is advanced at the distal region, resulting in periodic propagating waves of neural activity from the distal to proximal regions. The previous studies showed that odor stimuli change the LFP frequency and the wave propagation speed. In this article, we review the previous studies, as well as our recent studies, on the spatiotemporal neural activities of the land slug *Limax* using fluorescent-imaging technique.

**Keywords:** land slug, olfactory processing, spatiotemporal neural activity, fluorescent-imaging technique, voltage-sensitive dye, calcium-sensitive dye

---

## 1. Introduction

The conventional electrophysiological methods have been well used for the measurement of neural activities of vertebrate and invertebrate. The direct measurement from single neurons and neural areas is possible by the conventional methods using microelectrodes. However, the brain or central nervous system forms a network composed of so many neurons and

their function is based on complex interactions among electric neural activities, intracellular calcium signals, intercellular communications by neurotransmitter, etc. The electrophysiological methods are not suitable for the simultaneous measurement from many neurons or neural areas. For multi-point measurement of neural activities, fluorescent-imaging technique using voltage-sensitive dyes or calcium-sensitive dyes can be a powerful technique. In this technique, the dyes, which change their fluorescent intensities due to the voltage or calcium ion concentration change [1], are loaded into the cells, and their fluorescence changes are acquired into a computer as a series of images.

The multi-point measurement using fluorescent-imaging technique has been reported in vertebrates [2–5] and invertebrates [6–16]. In invertebrates, for example, this technique has been applied to measure spatiotemporal neural activities involved in the olfactory processing of the land slug *Limax* [6, 7, 9–11, 13–16]. In *Limax*, the procerebral (PC) lobe, which is the olfactory center located in the lateral part of each cerebral ganglion, spontaneously produces a periodic oscillation of local field potential (LFP) of about 1 Hz. The LFP oscillation is well synchronized over the entire PC lobe, but the phase of oscillation is advanced at the distal region, resulting in periodic propagating waves of neural activity from the distal to proximal regions. The previous studies showed that odor stimuli change the LFP frequency and the wave propagation speed.

In this article, we review the previous studies, as well as our recent studies, on the spatiotemporal neural activities of the land slug *Limax* using fluorescent-imaging technique.

## 2. Fluorescent-imaging technique

In fluorescent-imaging technique, the dyes, which change their fluorescence intensities due to the voltage or calcium ion concentration change [1], are loaded into cells, and their fluorescence changes are acquired into a computer as a series of images. However, the voltage-sensitive dyes generally exhibit a relatively small change in the fluorescence intensities, resulting in a low signal-to-noise (S/N) ratio. On the other hand, the calcium-sensitive dyes exhibit a larger change in the fluorescence intensities than that of the voltage-sensitive dyes. Therefore, their fluorescence changes can be detected easily, which enables us to indirectly measure neural activities because the intracellular calcium concentration often increases with neural activities.

As the calcium-sensitive dyes, those bonded with the acetoxymethyl (AM) group are commonly used because they are permeable into cells. After the AM-bonded dyes permeate into cells, the AM group is dissociated by intracellular esterase, and then the dyes can be non-permeable and loaded into cells. Vertebrate neurons are well known to be easily loaded with the AM-bonded calcium-sensitive dyes. In invertebrates, however, the AM-bonded dyes cannot be easily loaded into neurons because the AM group is difficult to be dissociated due to their weak activity of intracellular esterase.

For these reasons, it has not been determined yet which type of dyes is better for fluorescent imaging of neural activities in invertebrates. In Section 4, we introduce some studies on the

spatiotemporal neural activities of the land slug *Limax* using fluorescent-imaging technique with both types of dyes.

### 3. Neural systems for olfactory processing of the land slug

The land slug *Limax* has two pairs of tentacles, the superior and inferior tentacles. **Figure 1** shows a photograph of the central nervous system of *Limax* and the schematic illustration of the cerebral ganglion and superior tentacle. Each tentacle has an olfactory epithelium, which receives odors, at its tip. Olfactory receptor neurons are located at the tip regions of the digitate extensions of the tentacular ganglion (TG) (referring as “digitate ganglion” in **Figure 1B**) beneath the epithelium and terminate to synapse projection neurons in the TG that is the primary center of olfactory information processing (**Figure 1B**). The TG contains interneurons, as well as projection neurons that project to the cerebral ganglion [17]. The TG shows a spontaneous oscillation of LFP at about 2 Hz, which is usually measured by extracellular recording [18]. The oscillation is modulated by odor and air stimuli [19]. Several neurotransmitters such as serotonin, acetylcholine, glutamate, and gamma-aminobutyric acid (GABA), exist in the TG and modulate the spontaneous oscillation [20–22]. In addition, the olfactory epithelium also shows an oscillatory electro-olfactogram (EOG) in response to odor and air stimuli. The EOG oscillation interacts with the LFP oscillation in the TG [19].

TG neurons project to the cerebral ganglion via the tentacle or olfactory nerves. The major target of projection is the procerebral lobe, which is the lateral part of the cerebral ganglion (**Figure 1**). The PC lobe is a division of the cerebral ganglion unique to terrestrial slugs and snails that is specialized for the processing of olfactory information [23–25]. The PC lobe consists of three layers, the cell mass (CM), terminal mass (TM), and internal mass (IM) (**Figure 2**). The CM contains a large number of cell bodies of neurons, which are generally

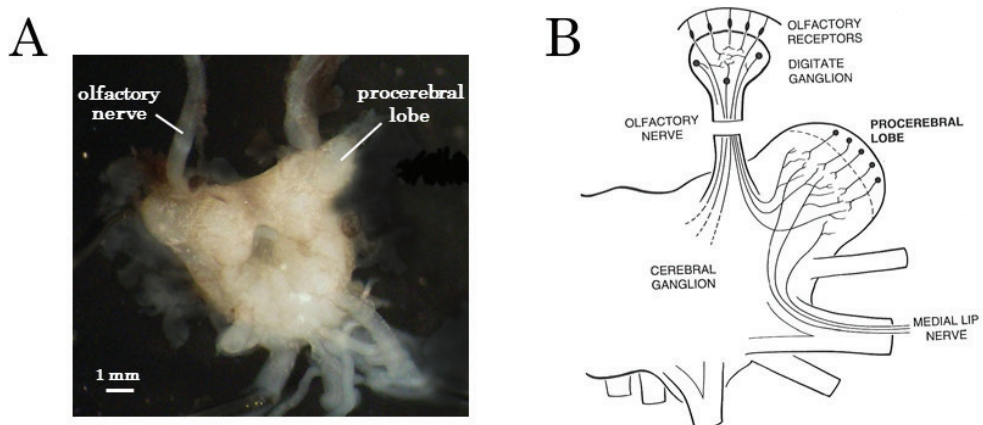


**Figure 1.** (A) Photograph of the central nervous system of the land slug *Limax* Color online and (B) schematic illustration of the cerebral ganglion and superior tentacle. This figure (B) is reproduced from Ref. [7] with permission.

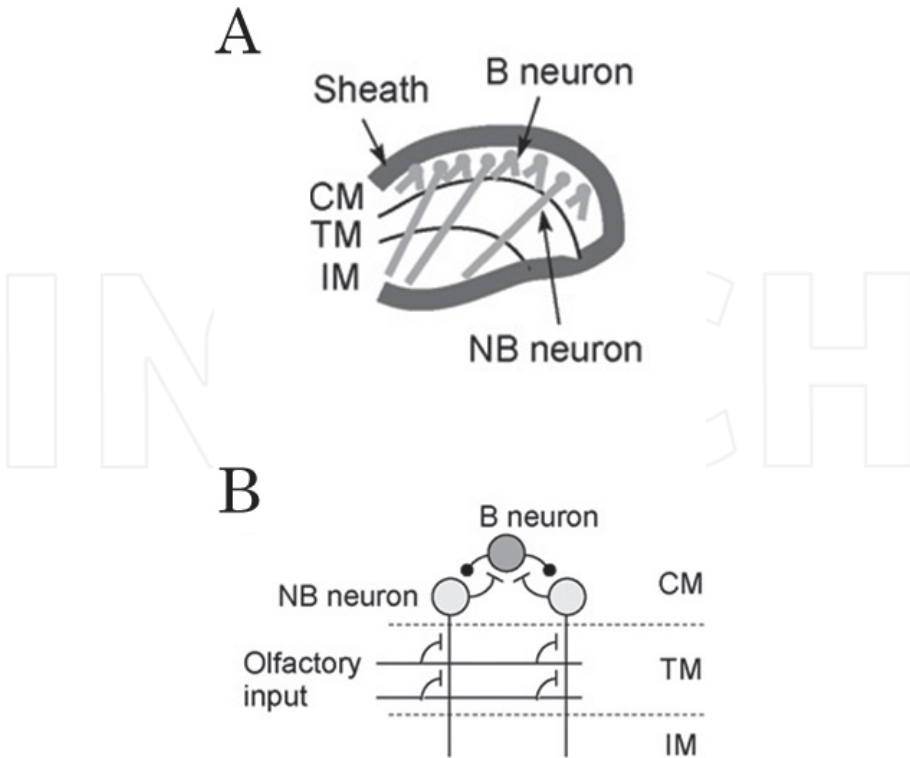


**Figure 2.** (A) Schematic illustration of the PC and (B) structure of the neural network of the PC. B neuron: bursting neuron, NB neuron: nonbursting neuron; CM: cell mass, TM: terminal mass, IM: internal mass. These figures are reproduced from Ref. [14] with permission.

small (5–8  $\mu\text{m}$ ) [23]. The TM and IM are neuropile layers. The TM receives input from the tentacle nerves [9]. The PC lobe spontaneously produces a periodic slow oscillation of LFP at about 1 Hz, which is usually measured by extracellular recording [26]. The LFP oscillation is well synchronized over the entire PC, but the phase of the oscillation is advanced at the distal region. This results in periodic propagating waves of neural activity from the distal to proximal regions, which has been clearly shown by fluorescent-imaging technique [6, 7, 9–11, 13–16].

Patch-clamp recording from single neurons showed that the neurons in the PC lobe are categorized as either bursting (B) or nonbursting (NB) neurons [6, 7] (**Figure 2**). B neurons are characterized by periodic bursting activity, and NB neurons are silent or fire at a low frequency. NB neurons are more numerous (about 90%) and have projection of neurites to the TM and IM [27]. NB neurons receive olfactory input from the tentacle nerves in the TM [28]. B neurons have extensive projection of neurites within the CM and inhibit NB neurons, while NB neurons excite B neurons. The spontaneous bursting activities of B neurons and inhibitory synaptic potentials in NB neurons are synchronized with the LFP oscillation.

The propagating waves of neural activity have also been found in mammalian cortex. However, the function and computational role are still unclear even in the land slug *Limax*. To elucidate it, fluorescent-imaging technique is expected to be a powerful technique as described in the subsequent section.

#### 4. Fluorescent imaging of spatiotemporal neural activities involved in the olfactory processing of the land slug

As mentioned earlier, periodic waves of neural activity propagate from the distal to proximal regions in the PC lobe of the land slug *Limax*. Pioneer works of a group clearly showed this phenomenon for the first time in the PC lobe of *L. maximus* by fluorescent voltage imaging using a voltage-sensitive dye [6, 7]. They used di-4-ANEPPS, a substituted aminonaphthylethenyl-pyridinium [29], as the fluorescent voltage-sensitive dye. The fluorescence was detected with either an array of photodiodes or a cooled charge-coupled device (CCD) camera. **Figure 3** shows the experimental apparatus that they used. **Figure 4** shows the propagating waves of fluorescence change measured by the CCD camera. A band of depolarization, followed by a band of hyperpolarization, began at the distal tip and moved along the length of the PC lobe, resulting in a phase difference between the distal and proximal regions (**Figure 4A** and **C**). The detailed shape of the optical signal as a function of time also varied between different regions (**Figure 4B**). Simultaneous recording of the optical signal and the LFP by extracellular recording showed that the oscillatory changes in the fluorescent intensity were synchronized to the LFP oscillation (**Figure 5**). Additionally, from simultaneous recording of the optical signal and the intracellular potential by whole-cell patch technique (**Figure 6**), the authors concluded that the major part of the optical signal can be interpreted as a superposition of the intracellular signals arising from the B and NB neurons.

They next examined the responses of spatiotemporal neural activity in the PC lobe to odor stimuli (**Figure 7**). The stimuli were applied to the epithelium of the superior tentacle. The phase difference of neural activity between the distal and proximal regions was not changed in response to the moist air (**Figure 7A**). However, in response to a component of natural potato odor (2-ethyl-3-methoxypyrazine; EMOP), a known appetitive stimulus to the naïve slugs, the phase difference was dramatically changed (**Figure 7B–F**). The stimulus caused a collapse of the phase difference, that is, an initial difference of  $\Delta t > 250$  ms was reduced to  $\Delta t < 50$  ms. Repeated stimulus also caused a collapse of the phase difference, although it recovered faster after cessation of the stimulus. The transient switch from the states with propagating waves to one with spatially uniform oscillations is hypothesized to allow nearest-neighbor interactions suppressed by the propagating wave activity [30]. This study suggested that olfactory information is encoded in the spatiotemporal neural activities in the PC lobe.

Thereafter, other groups have also studied the spatiotemporal neural activities of the PC lobe using fluorescent voltage imaging. Kimura et al. examined the responses of the PC lobe of *L. marginatus* to aversively conditioned odors [10]. In this study, di-4-ANEPPS was also used as the voltage-sensitive dye. First, they performed aversive conditioning procedures to the slugs using two odors (carrot and cucumber, which strongly attract the naïve slugs)

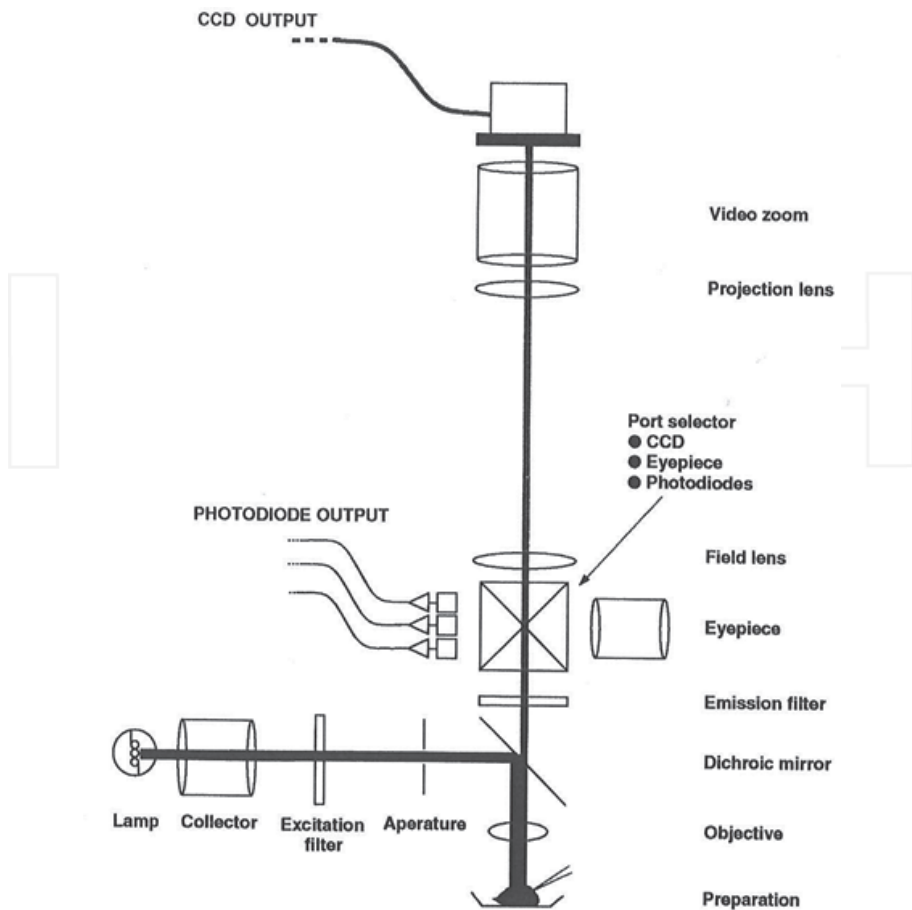


**Figure 3.** Schematic illustration of the experimental apparatus used for the optical measurement. This figure is reproduced from Ref. [7] with permission.

as conditioned stimuli (CS) and quinidine sulfate solution, which induces a strong aversive effect, as an unconditioned stimulus (UCS). The odor stimuli were applied to the epithelium of the inferior tentacle. When the conditioning is completed, the slugs avoid the CS odor and exhibit eating behavior at a lower frequency [31]. In the PC of the naïve slugs, they observed the propagating waves of fluorescence change similar to those reported in the previous study [6, 7] (**Figure 8**). In the PC lobe of the slugs aversively conditioned by carrot odor, the instantaneous frequency of the oscillatory fluorescence change was decreased from about 4 s after the onset of conditioned carrot odor presentation (**Figure 9a**). The optical signals recorded in an area of the PC lobe (area 3 in the upper image of **Figure 9**) showed depolarization in the basal potential (bottom level of each cycle of the oscillation) immediately after the onset of the odor presentation (**Figure 9d**). In another area of the PC lobe (area 4 in the upper image of **Figure 9**), hyperpolarization in the basal potential occurred from about 5 s after the carrot



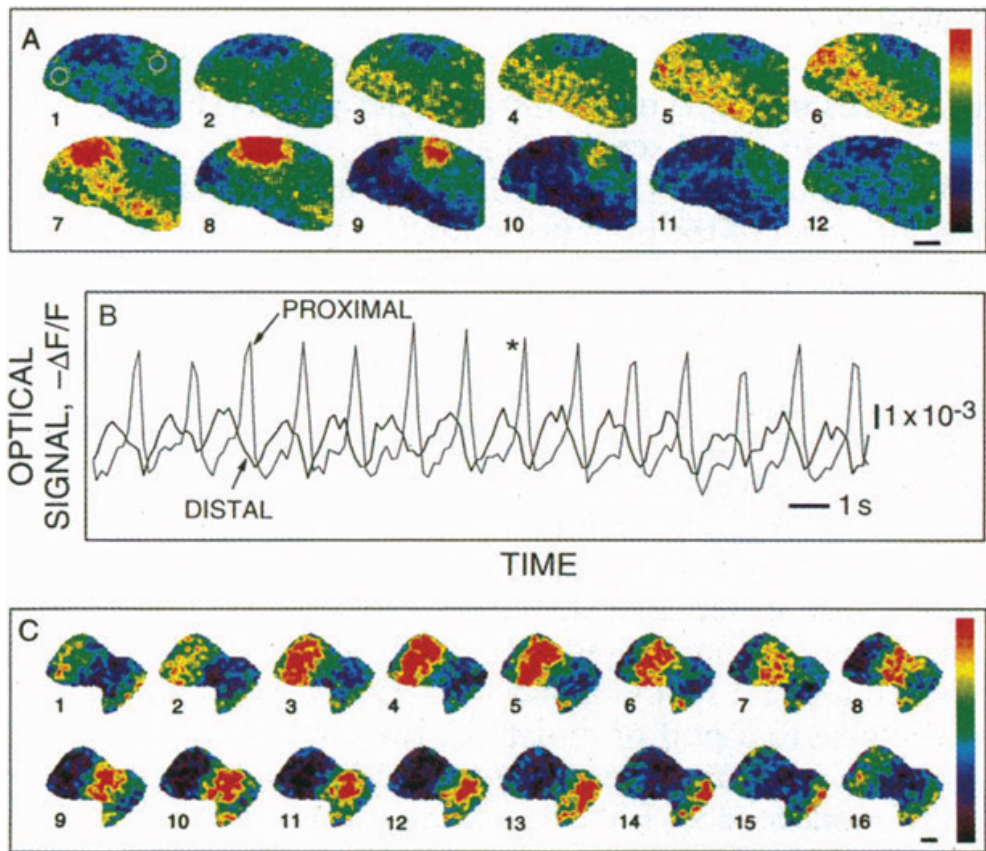


**Figure 4.** Propagation waves of fluorescence change in the PC lobe Color online. (A) Lateral view of fluorescence changes ( $-\Delta F/F$ ) plotted as successive frames. The fluorescence images were acquired as  $100 \times 100$  pixel images at a frame rate of 120 ms. The scale bar shows  $100 \mu\text{m}$ . (B) Fluorescence changes versus time for the distal (thick line) and proximal (thin line) regions in the lobe. Each signal is the average signal from each circled region in (A). The asterisk (\*) corresponds to frames 8 in (A). (C) Posterior view of fluorescence changes. The fluorescence images were acquired as  $100 \times 100$  pixel images at a frame rate of 112 ms. The scale bar shows  $100 \mu\text{m}$ . In (A) and (C), yellow/red indicate depolarization and blue/violet indicate hyperpolarization relative to the average voltage. These figures are reproduced from Ref. [6] with permission.

odor presentation (**Figure 9e**). On the other hand, the control cucumber odor did not significantly induce those changes (**Figures 9f–j**). **Figure 10** shows temporally average images of optical signals calculated in 10 different periods of two recordings shown in **Figure 9** (periods a–j in the upper graphs of **Figure 10**). This result shows that depolarization occurred especially in the neurons located in a belt-shaped region of the middle of the PC lobe (red-colored region in image b in **Figure 10**) immediately after the onset of conditioned carrot odor presentation. The belt-shaped region corresponded to area 3 in the upper image of **Figure 9**, in which depolarization in the basal potential occurred in the time profile, while the early phase depolarization was not observed for the control odor cucumber. After the depolarization was diminished, hyperpolarization occurred in the neurons in a relatively wide area of the PC lobe

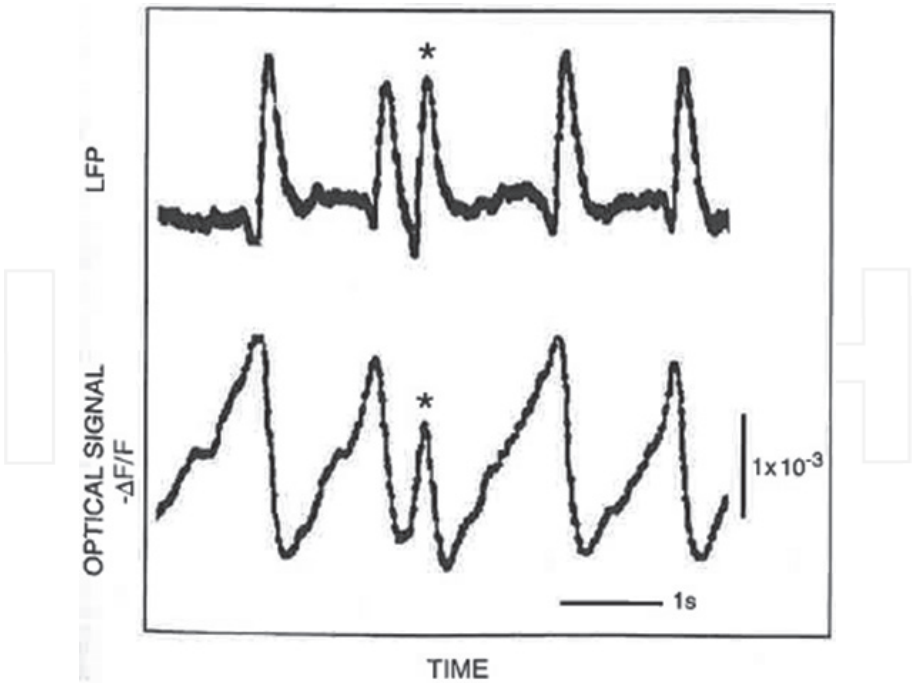


**Figure 5.** Simultaneous recording of the optical signal and the LFP by extracellular recording from a mid-distal region in the PC lobe. The asterisk (\*) shows a “double event” that simultaneously presents in both recordings. This figure is reproduced from Ref. [7].

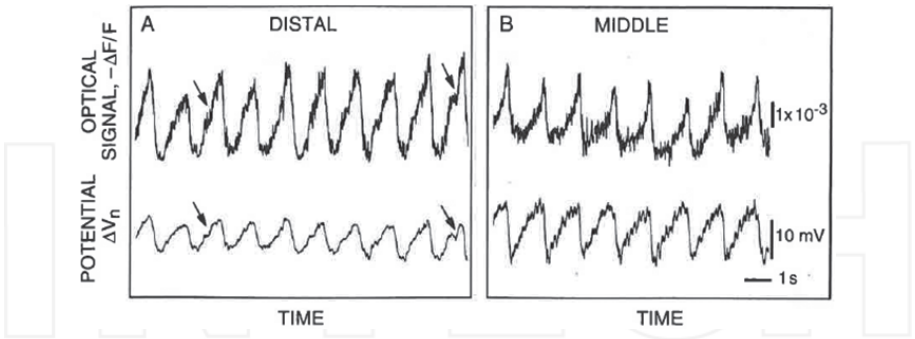


**Figure 6.** Simultaneous recording of the optical signal and the intracellular potential by whole-cell patch technique. (A) Recording from the distal region in the PC lobe. Two pairs of arrows show “fast events” that are simultaneously present in both recordings. (B) Recordings from the middle region in the PC lobe. These figures are reproduced from Ref. [7].

(blue-colored region in images c and d in **Figure 10**). Similar results were obtained in the PC lobe of the slugs aversively conditioned by cucumber odor. From these results, the authors concluded that in the PC lobe, learned odors are represented as spatiotemporal activity patterns, which is supported by activity-dependent dye uptake study [32].



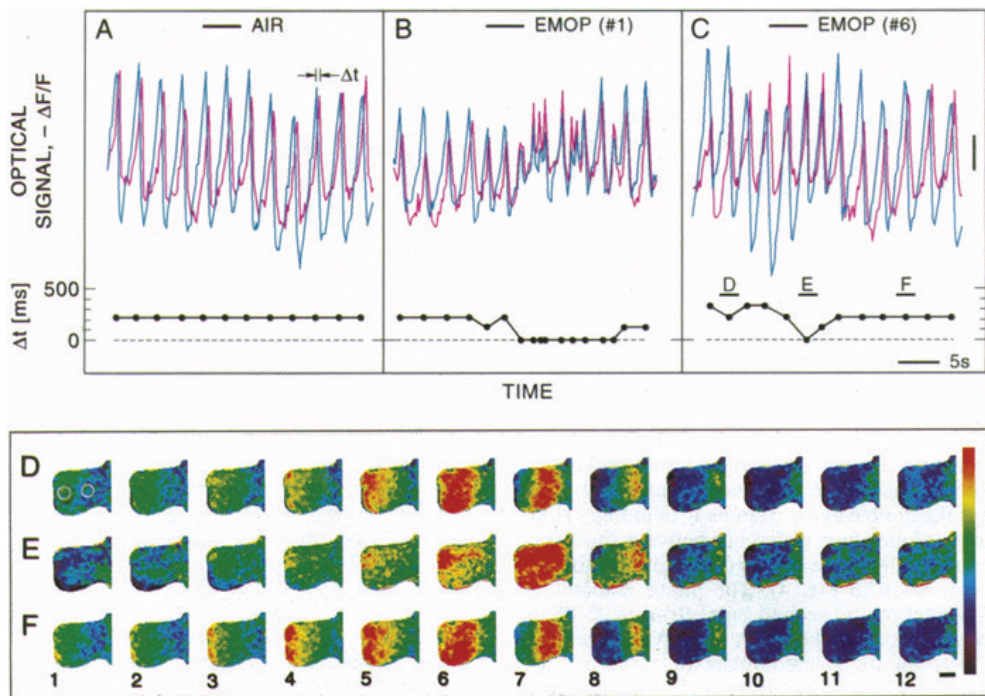


**Figure 7.** Fluorescent optical recordings of neural activity in the PC lobe in response to natural odor stimuli Color online. (A) Fluorescence changes ( $-\Delta F/F$ ) versus time during the exposure to moist air (bar mark). The changes are shown for the distal (blue line) and proximal (red line) regions indicated by the circles in (D). (B) Fluorescence changes ( $-\Delta F/F$ ) versus time during the first exposure to EMOP (bar mark). (C) Fluorescence changes ( $-\Delta F/F$ ) versus time during the sixth exposure to EMOP (bar mark). Each lower plot in (A)–(C) shows the time difference ( $\Delta t$ ) between successive peaks in the optical signal for each period. (D–F) Images of the fluorescence changes corresponding to the data in (C). They were taken (D) prior, (E) during, and (F) after the odor stimulation, which correspond to the letters D–F in (C). The fluorescence images were acquired as  $100 \times 100$  pixel images at a frame rate of 112 ms. The scale bar shows 100  $\mu\text{m}$ . These figures are reproduced from Ref. [6] with permission.

Watanabe et al. measured neural activities of other areas in the cerebral ganglion, metacerebrum/mesocerebrum (MC) (**Figure 9**), together with the PC lobe by fluorescent voltage imaging, and they analyzed the relationship between them using the correlation analysis [13]. In this study, di-4-ANEPPS was also used as the voltage-sensitive dye. **Figure 11** shows the fluorescent optical recording of spontaneous activity of the cerebral ganglion of *L. valentianus*. The image field covered the proximal part of the PC and the entire ipsilateral MC region. In all preparations, they observed oscillatory neural activity in the PC. Additionally, they found clear oscillatory activity in the MC with the same frequency as the PC oscillation in some preparations, although the amplitude of the MC oscillation was smaller than that of the PC oscillation. Their phase relationship was variable. In some preparations, the two oscillations were antiphase, while in the other preparations the oscillations were inphase. This study indicated that the oscillatory activity in the PC lobe, in which olfactory information is encoded as mentioned earlier, propagates to the MC that plays a role in motor command.

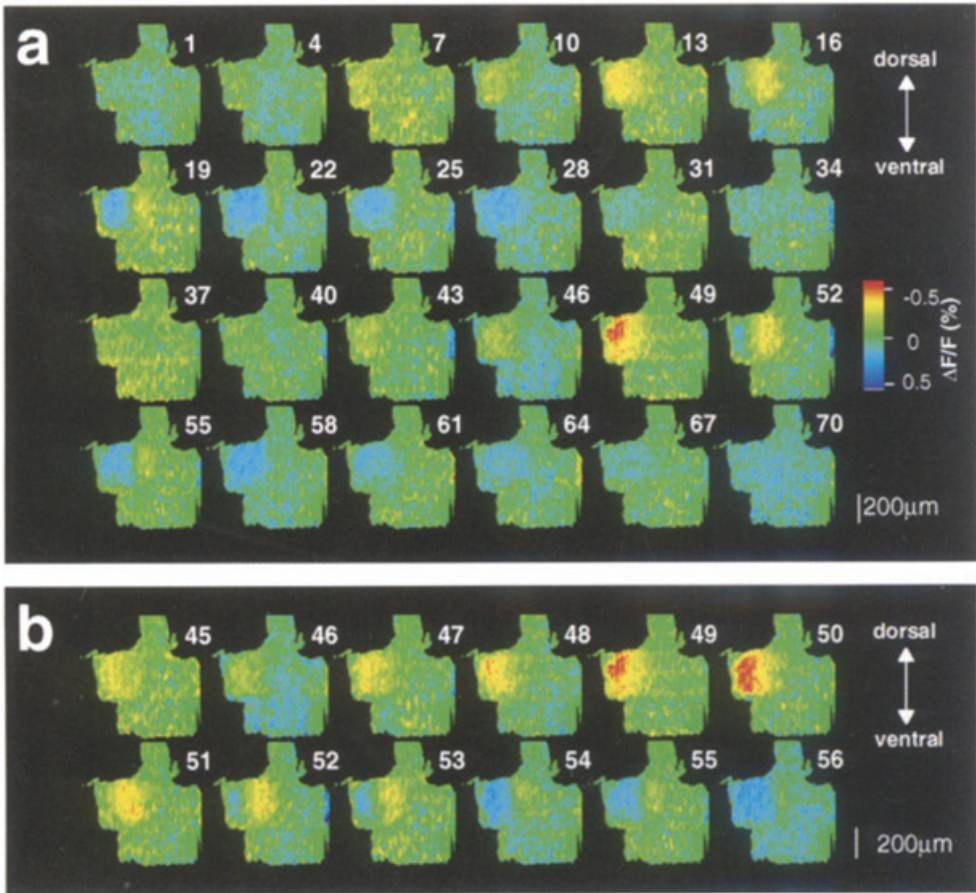


**Figure 8.** Propagation waves of fluorescence change in the PC lobe (posterior view) Color online. The fluorescence images were acquired by a photodiode array as  $128 \times 128$  pixel images at a frame rate of 38.4 ms. Fluorescence changes ( $\Delta F/F$ ) were plotted as successive frames. The  $\Delta F/F$  value in each pixel is represented according to the color table. (a) Frames 1–70 with an interval of 115.4 ms. (b) Frames 45–56 with an interval of 38.4 ms. These figures are reproduced from Ref. [10] with permission.

The spatiotemporal neural activities in the PC lobe were also measured by fluorescent calcium imaging using calcium-sensitive dyes. Inoue et al. used Oregon Green-1, rhod-2, or Ca Orange bonded with AM group as the calcium-sensitive dye, and compared the fluorescent calcium imaging using each of them with the fluorescent voltage imaging using di-4-ANEPPS [11]. In fluorescent calcium imaging, propagation waves of fluorescence change were also observed in the PC lobe of *L. marginatus* (**Figure 12**). The PC lobe was well stained by the calcium-sensitive dyes, even though AM group-bonded dyes were used. The calcium signals originated predominantly from the cell body layer, CM, while the voltage signals originated mainly from the neurophil layer, TM. The calcium-sensitive dyes gave 1–3% fluorescence change, which increased rapidly and decreased slowly, with a good signal-to-noise ratio (**Figure 13**). Among the calcium-sensitive dyes, rhod-2 gave the largest fluorescence oscillation. On the

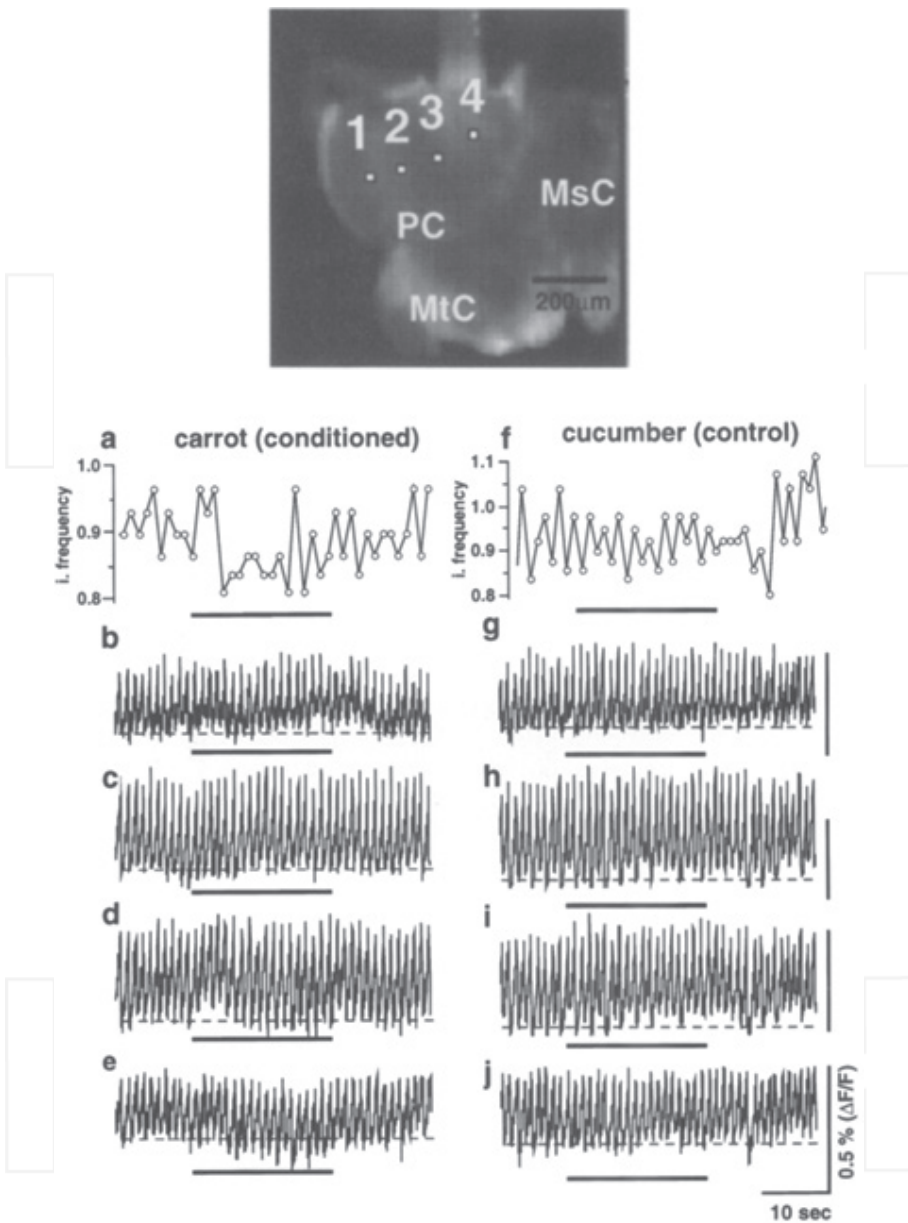


**Figure 9.** Olfactory responses in the fluorescence oscillation in the PC lobe. The preparation was isolated from a slug aversively conditioned by carrot odor. The optical signals were recorded from four regions (open squares 1–4 in the upper image) of the posterior surface. (a) Change in the oscillation frequency induced by conditioned carrot odor. (b–e) Fluorescence changes ( $\Delta F/F$ ) versus time during the exposure to carrot odor (bar mark). (f) Change in the oscillation frequency induced by control cucumber odor. (g–j) Fluorescence changes ( $\Delta F/F$ ) versus time during the exposure to cucumber odor (bar mark). (b) and (g), (c) and (h), (d) and (i), and (e) and (j) correspond to regions 1–4 in the upper image, respectively. MtC: metacerebrum, MsC: mesocerebrum. These figures are reproduced from Ref. [10] with permission.

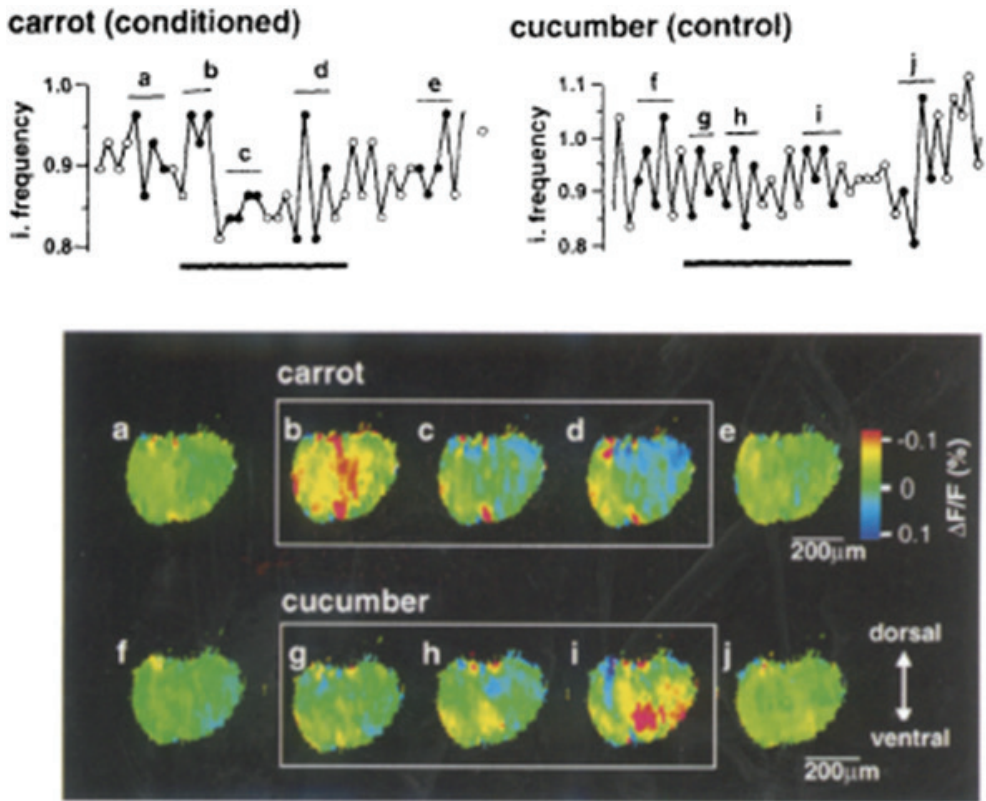


**Figure 10.** Spatiotemporal properties of olfactory responses in the PC lobe Color online. The upper two graphs show responses of the oscillation frequency to aversively conditioned carrot odor (left) and control cucumber odor (right). The lower images show temporally averaged  $\Delta F/F$  images calculated from the optical recording shown in Figure 9. Successive images were averaged for 10 different periods (a–j in the upper figures, each of which includes three or four oscillatory cycles (•)). The images a–j corresponds to the periods a–j. These figures are reproduced from Ref. [10] with permission.

other hand, the voltage-sensitive dye gave 0.1–1% fluorescence change, which increased slowly and decreased rapidly (**Figure 13**). In this study, the authors concluded that the oscillatory signals of the calcium-sensitive dyes arise from B neurons of the CM and the neural activity of the CM can be monitored with them because the oscillatory signals were synchronized with the LFP (**Figure 13**).

Fluorescent calcium imaging has been limited with respect to the selectivity of staining of the dyes. Bath application of the dyes stains both B neurons and NB neurons. Even when we intend to observe the activity of NB neurons, which is thought to be involved in odor coding [33], it is obscured by stronger calcium signals from B neurons that exhibit periodic bursting activity. To observe the activity of NB neurons, Watanabe et al. attempted selective fluorescent calcium imaging for the PC lobe of *L. valentianus* by retrograde staining of NB neurons with rhod-2 [14]. When the sheath was removed only from the surface of the IM and the PC lobe was immersed in the dye solution, the NB neurons were expected to be stained



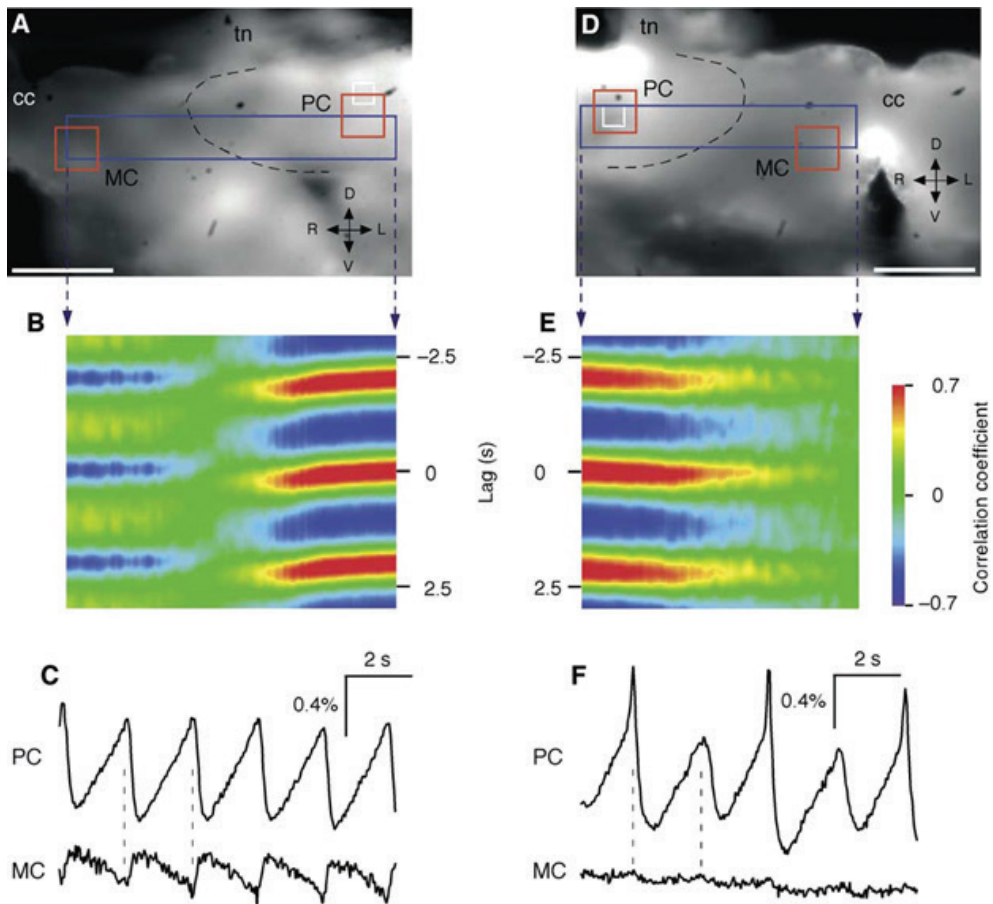


**Figure 11.** Fluorescent optical recording of spontaneous activity in the cerebral ganglion Color online. (A–C) A preparation that showed an antiphase MC oscillation. (A) Fluorescent image of the cerebral ganglion (left hemisphere) observed from the anterior surface. The scale bar shows 200  $\mu\text{m}$ . tn: superior tentacle nerve, cc: cerebral commissure; D: dorsal, V: ventral, L: left, R: right. The broken line around the PC indicates the border between the PC and the MC. (B) Correlation profile along the area indicated by the blue rectangle in (A), with reference to the PC region (white square). The horizontal axis corresponds to the position along the area, and the vertical axis is the time lag. Positive values of the lag indicate delays relative to the PC. Pseudocolor presentation (the table on the right of (E)) refers to the amplitude of correlation against the PC oscillation. (C) Fluorescence changes versus time in the PC and MC regions indicated by the red squares in (A). Decrease in fluorescence intensity (depolarization of the membrane potential) is plotted upward. As the dotted lines indicate, the two traces show an antiphase relationship. (D–F) A preparation that showed an inphase MC oscillation. (D) Fluorescent image of the cerebral ganglion (right hemisphere) observed from the anterior surface. The scale bar shows 200  $\mu\text{m}$ . Abbreviations are same as those in (A). The broken line around the PC indicates the border between the PC and the MC. (E) Correlation profile along the area indicated by the blue rectangle in (D), with reference to the PC region (white square). (F) Fluorescence changes versus time in the PC and MC regions indicated by the red squares in (D). As the dotted lines indicate, the two traces show an inphase relationship although the amplitude of the MC oscillation is small. These figures are reproduced from Ref. [13] with permission.

retrogradely through neurites projected to the IM (**Figure 14**). After nonselective staining, in which the sheath was removed from the entire surface of the PC lobe, a strong spontaneous oscillation was observed, which presumably arose from calcium oscillations of B neurons

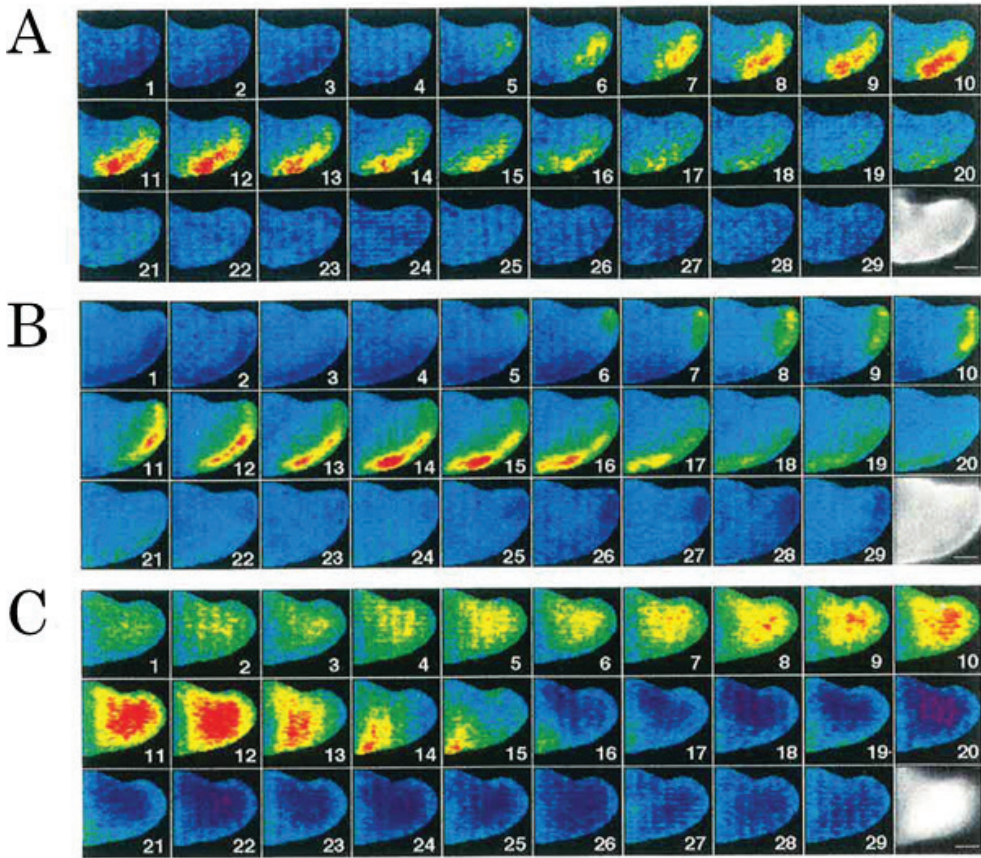


**Figure 12.** Propagation waves of fluorescence change in the PC lobe (dorsal view) stained with (A) Oregon Green-1, (B) rhod-2, or (C) di-4-ANEPPS Color online. The fluorescence images were acquired by a photodiode array as  $128 \times 128$  pixel images at a frame rate of 38.4 ms. In (A) and (B), yellow/red indicates high calcium concentration and blue/violet indicates low calcium concentration. In (C), yellow/red indicates depolarization, and blue/violet indicates hyperpolarization. The scale bar shows 200  $\mu\text{m}$ . These figures are reproduced from Ref. [11] with permission.

(Figure 15). On the other hand, the PC lobe showed a much smaller spontaneous oscillation after the selective staining, although a large number of cells were clearly stained (Figure 15). This result suggested that NB neurons are mostly silent in contrast to B neurons. However, NB neurons responded to electric stimulation of the superior tentacle nerve as shown in the inset of Figure 15D.

As described above, fluorescent-imaging technique is applicable for the measurement of the spatiotemporal neural activities involved in the olfactory processing of the land slug. Through the studies using it, especially, the function and computational roles of the propagation waves of neural activity in the PC lobe on odor discrimination and learning have been elucidated. Meanwhile, the experimental apparatus has also been improved. In the earlier reports of the fluorescent voltage imaging, consecutive images were acquired at a frame rate of about 100 ms



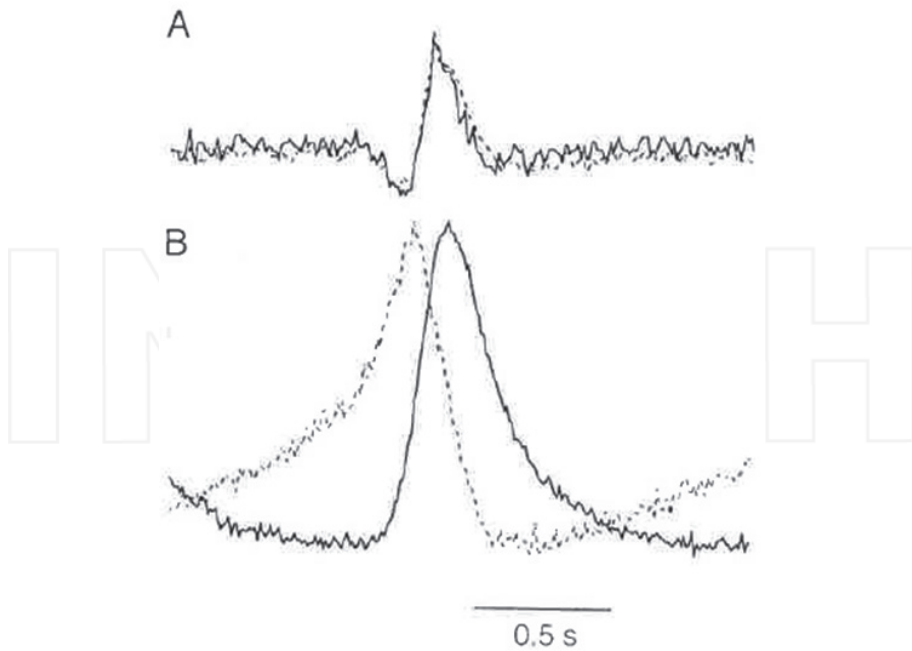


**Figure 13.** Phase relationship between the fluorescence oscillations of the calcium-sensitive dye (rhod-2) and the voltage-sensitive dye (di-4-ANEPPS) in the PC lobe. (A) LFP measured simultaneously with the optical recordings of the PC lobe stained with rhod-2 (solid line) or di-4-ANEPPS (dotted line). (B) Fluorescence changes of rhod-2 (solid line) and di-4-ANEPPS (dotted line) versus time. The fluorescence intensities were obtained by averaging over  $10 \times 10$  pixels at the medial region of the CM. These figures are reproduced from Ref. [11] with permission.

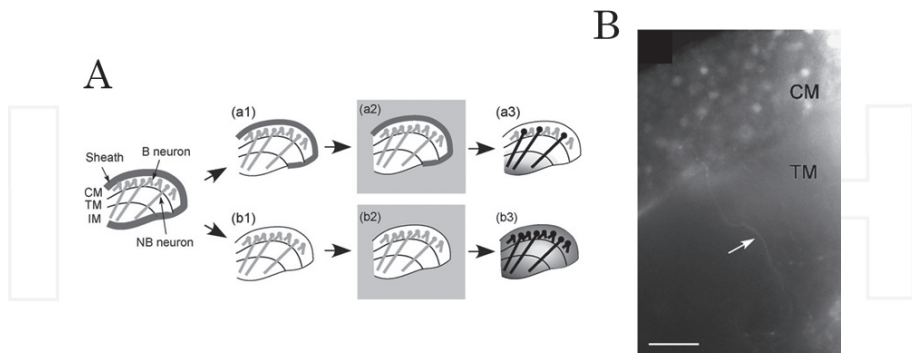


**Figure 14.** (A) Methods of staining. (a1–3) Selective staining of NB neurons. (a1) The sheath is removed only from the surface of the IM. (a2) The preparation is incubated in the rhod-2 solution. (a3) After staining, NB neurons but not B neurons are stained. (b1–3) Nonselective staining. (b1) The sheath is removed from the entire surface of the PC. (b2) The preparation is incubated in the rhod-2 solution. (b3) After staining, both B and NB neurons are stained. (B) Fluorescence image of a section of the PC lobe after staining. Cell bodies (bright spots) are stained in the CM. A neurite is also stained in the TM (arrow), through which the dye presumably diffused to stain the cell body. The scale bar shows 40  $\mu\text{m}$ . These figures are reproduced from Ref. [14] with permission.

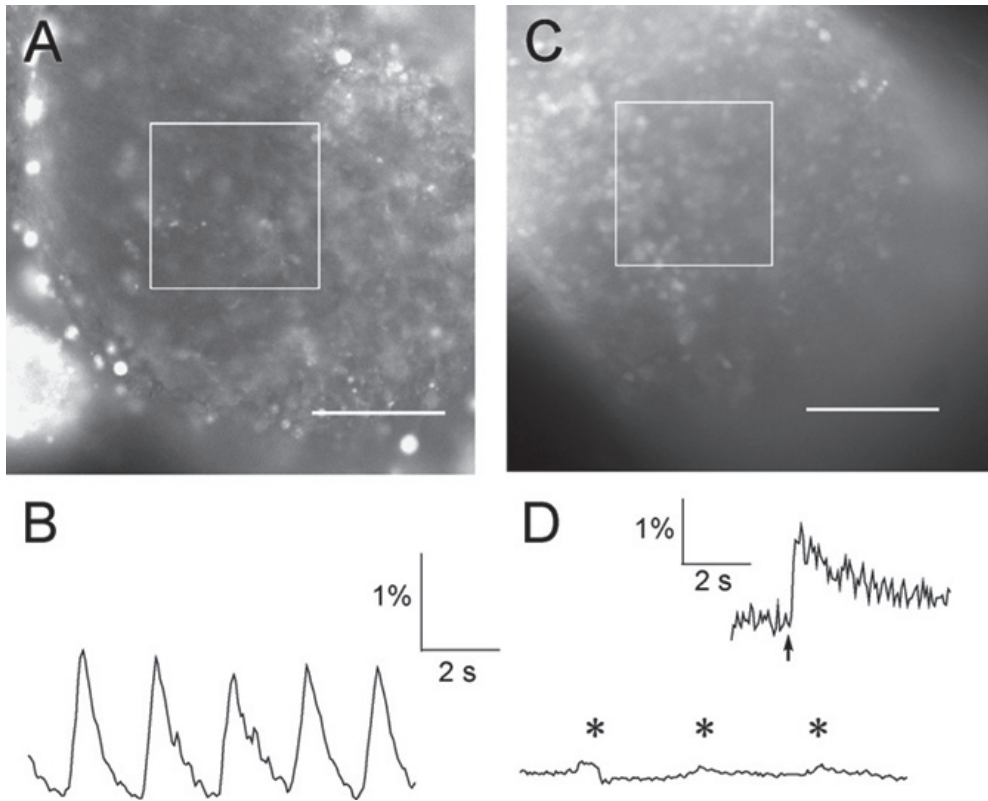


**Figure 15.** Comparison of selective and nonselective staining. Spontaneous activity was recorded from the surface of the CM in the PC lobe. (A and B) Nonselective staining. (A) Fluorescence image of the surface of the CM. (B) Time course of the averaged fluorescence from the square region (approximately  $100 \times 100 \mu\text{m}$ ) in the center of (A). (C and D) Selective staining. (C) Fluorescence image of the surface of the CM. (D) Time course of the averaged fluorescence from the square region (approximately  $100 \times 100 \mu\text{m}$ ) in the center of (C). The inset shows the time course of fluorescence in a cell in response to electric stimulus of the superior tentacle nerve (arrow). The scale bars in (A) and (C) show  $100 \mu\text{m}$ . These figures are reproduced from Ref. [14] with permission.

for about  $100 \times 100$  pixels in size [6, 7], while they can be acquired at a frame rate of about 10 ms for about  $1000 \times 1000$  pixels in size in our recent apparatus as described in Section 5.

## 5. Our recent fluorescent-imaging apparatus and its application

We have also measured the spatiotemporal neural activities in the PC lobe of the land slug *Limax* by fluorescent voltage imaging [15, 16]. **Figure 16** shows our recent apparatus. We also use di-4-ANEPPS as the voltage-sensitive dye. The recording chamber, in which the stained preparation is placed, is mounted on the stage of a microscope (E-FN1, Nikon, Japan). The dye is excited by LED of 530 nm with a half width of 25 nm (LEX2-G, Brain Vision, Japan) through an excitation filter (EX510-560). The emitted fluorescence of 705 nm is detected through a dichroic

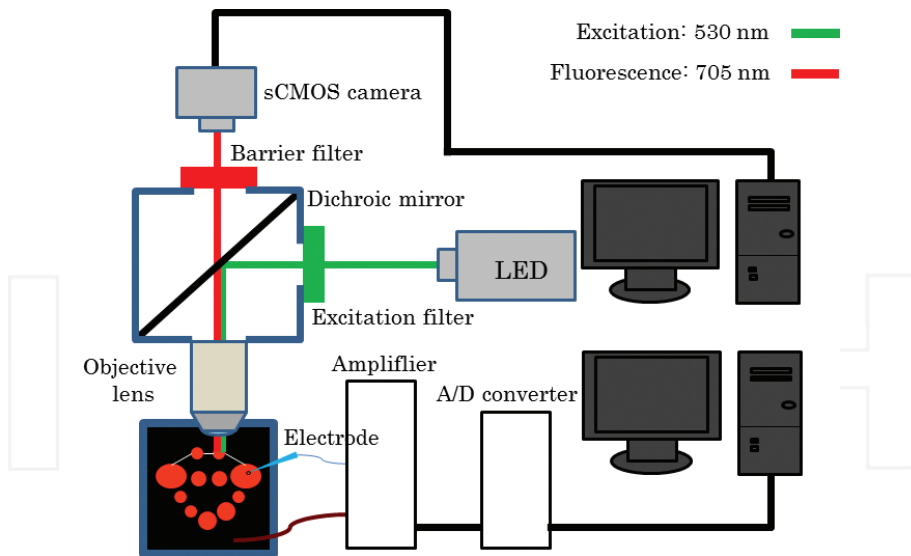


**Figure 16.** Schematic illustration of our recent fluorescent voltage-imaging apparatus Color online. The LFP can be simultaneously measured by extracellular recording. This figure is reproduced from Ref. [16] with permission.

mirror (DM575) and a barrier filter (BA590). The fluorescence images ( $1024 \times 1024$  pixels) are acquired at a frame rate of 10 ms by sCMOS camera (Zyla, Andor, Ireland). The acquired image sequences were stored into a personal computer (Dell Precision T5600, Dell, USA).

**Figure 17** shows the propagating waves of fluorescence change in the PC lobe of *L. valentianus* measured by our apparatus. The supplemental movie can be seen in the website (the URL is in the figure legend of **Figure 17**). Here, a  $10\times$  objective was used and the space resolution was about  $0.6 \mu\text{m}/\text{pixel}$ . An aversive odor, isoamyl acetate, was applied to the epithelium of

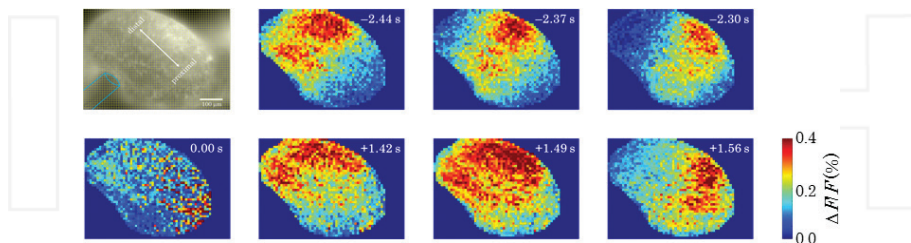


**Figure 17.** Propagation waves of fluorescence change in the PC lobe (upper left fluorescence image) measured by our recent apparatus Color online. The fluorescence images were acquired by a sCMOS camera as  $1024 \times 1024$  pixel images at a frame rate of 10 ms. The space resolution was about  $0.6 \mu\text{m}/\text{pixel}$ . Fluorescence changes ( $\Delta F/F$ ) were plotted as successive frames. The  $\Delta F/F$  values averaged over  $16 \times 16$  pixels (yellow mesh in the upper left image) were represented according to the color table. The LFP was simultaneously measured by the glass electrode (blue figure in the upper left image). The odor (isoamyl acetate) was applied at 0.00 s, and the time before or after the odor stimulus is shown in each frame. See also the supplemental movie (<http://saitolab-chaos.com/Papers/Malacology/Supplemental-movie.html>; 1/4 speed reproduction).

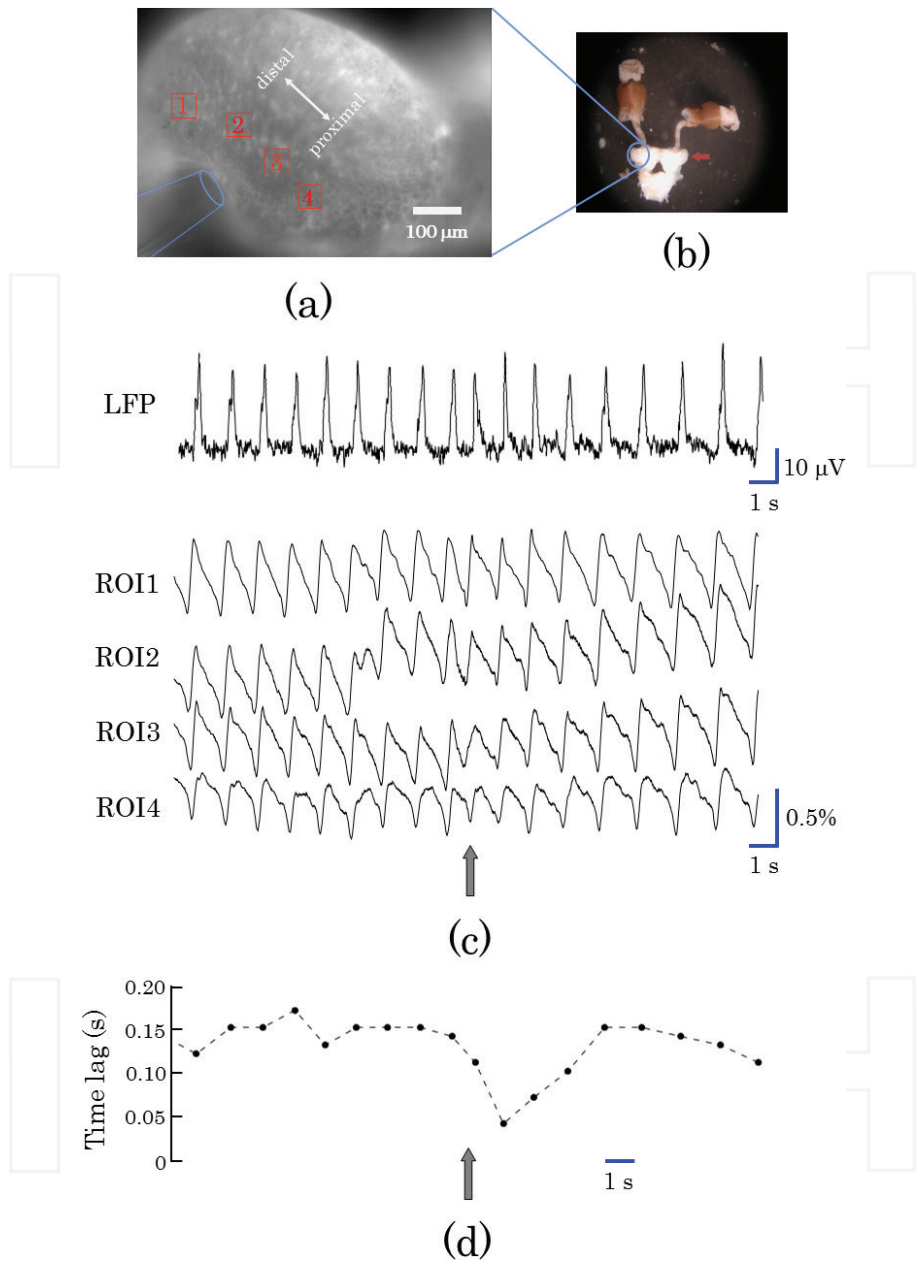


**Figure 18.** (a) Fluorescence image of the PC lobe Color online. The red squares (1–4) show the ROIs for fluorescence change analysis and the blue figure shows the glass electrode for LFP measurement. (b) Preparation of the central nervous system with tentacles. The blue circle and the red arrow show the left and right PC lobes, respectively. (c) Time courses of the LFP (upper figure) and the fluorescence change in the ROIs (lower figure). (d) Time lag estimated from the peaks of fluorescence oscillations in the ROI1 and ROI4. The odor (isoamyl acetate) was applied at the time shown by gray arrows in (c) and (d). These figures are reproduced from Ref. [16] with permission.

the superior tentacle. **Figure 18** shows the fluorescence changes in four ROIs. The time lag between two peaks at the distal and proximal regions significantly decreased, that is, the propagation speed significantly increased when the odor was applied. In our experiments, this phenomenon occurred only for the aversive odors, not for the appetitive odors.

We also examined the involvement of nitric oxide (NO) in the odor-induced changes in wave propagation by our apparatus. NO, which is a gaseous neurotransmitter, has been reported to function specifically in the PC lobe. Gelperin et al. showed that the excitability of B neurons is modulated by NO [34] and suppression of NO synthesis blocks the LFP oscillation and wave propagation in the PC lobe [35]. In our study [36], the stimulation of another aversive odor, hexanol, to the epithelium of the superior tentacle increased NO concentration measured by an NO electrode applied to the PC lobe of *L. valentianus*. This was blocked by NO synthase inhibitor L-NAME (3.7 mM), although it did not block the LFP oscillation and wave propagation in the PC lobe at this concentration. Additionally, the LFP frequency and wave propagation speed were increased by the odor (hexanol) stimulation or electrical stimulation of the superior tentacle nerve, and these phenomena also disappeared by L-NAME, but not by its inactive enantiomer D-NAME (**Figure 19**). On the other hand, L-NAME did not block synaptic transmission from the superior tentacle nerve to NB neurons in the PC lobe. These results suggested that NO is released from NB neurons diffuses into the CM to depolarize B neurons, which modifies the network activity, presumably the main effect of suppressing NB neurons (**Figure 20**). Based on this study as well as previous studies, the authors speculated that the effects of NO released during olfactory perception underlie the mechanism of precise odor discrimination and learning in the PC lobe of the land slug.

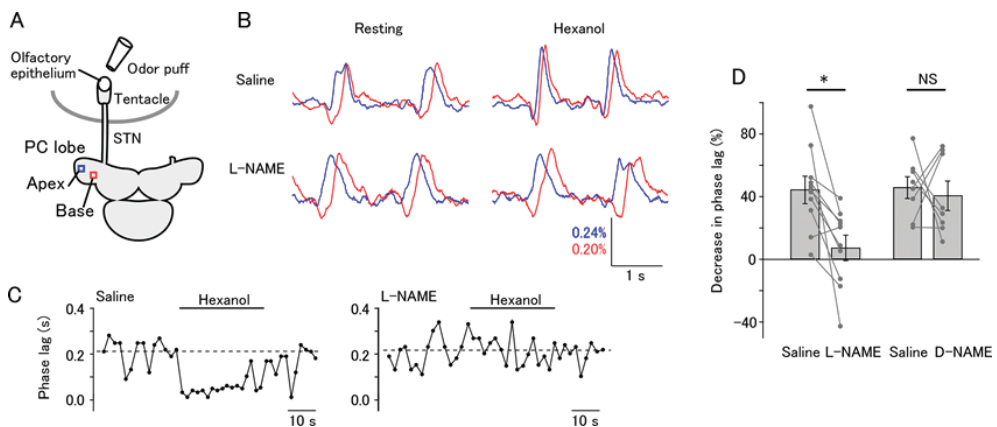


**Figure 19.** Effects of NO on the spatiotemporal neural activities in the PC lobe Color online. (A) Schematic illustration of the experiment. (B) Normalized fluorescence changes in the ROIs in the distal (apical) and proximal (basal) regions. Before the odor (hexanol) stimulation, the peaks of fluorescence changes had a time lag between the distal and proximal regions (upper left). The lag decreased during the odor stimulation (upper right). In the saline containing L-NAME, the odor stimulation did not decrease the lag (lower). (C) Time courses of the lag in saline (left) and L-NAME (right). The dotted lines indicate the average of lag before the stimulus. (D) Summary of the responses of lag to the odor stimulation. Average and individual data are shown. L-NAME significantly reduced the decrease in the lag ( $*p < 0.05$ ,  $N = 10$ ), whereas D-NAME did not significantly change the response (NS, not significant;  $N = 8$ ). These figures are reproduced from Ref. [36] with permission.

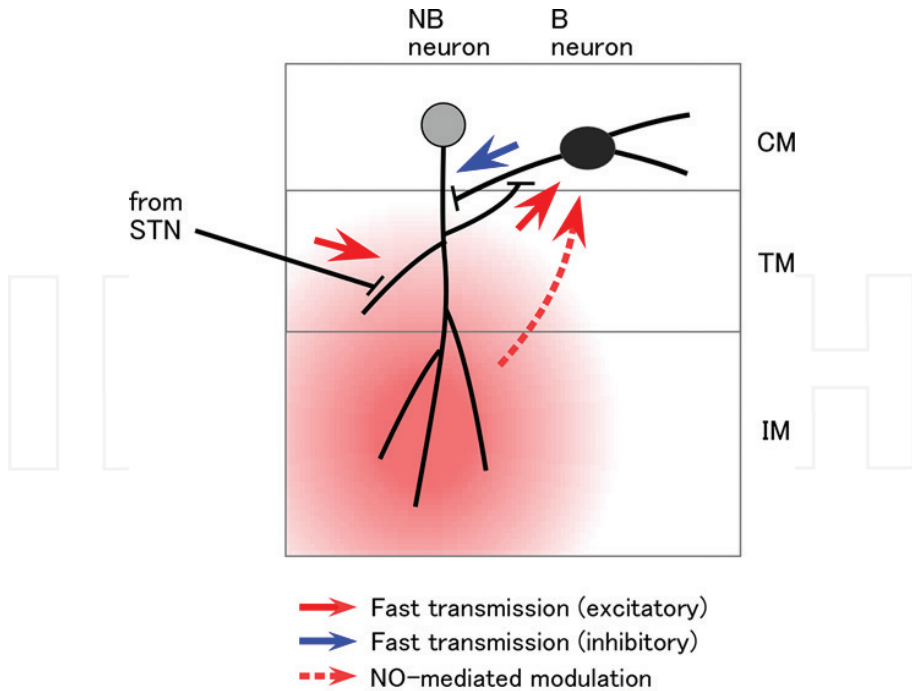


**Figure 20.** Schematic illustration of the pathways that transmit olfactory information to the PC lobe Color online. B and NB neurons have the cell bodies in the CM. The superior tentacle nerve projects in the TM and makes synapses on NB neurons. NB neurons produce spikes that propagate afferently and activate synapses on B neurons. At the same time, spikes also propagate efferently into the IM, where NO will be released. NO diffuses into the CM and depolarizes B neurons, which modifies the network activity, presumably by suppressing NB neurons. This figure is reproduced from Ref. [16] with permission.

6. Conclusions

Fluorescent voltage imaging is applicable for the measurement of the spatiotemporal neural activities involved in the olfactory processing of the land slug *Limax*. Fluorescent calcium imaging is also applicable for it, even though generally the AM group-bonded calcium-sensitive dyes cannot be easily loaded into invertebrate neurons. Through the studies using the fluorescent-imaging technique, especially, the function and computational roles of the propagation waves of neural activity in the PC lobe on odor discrimination and learning have been elucidated. Meanwhile, the experimental apparatus has also been improved. By our recent apparatus, consecutive images can be acquired at a flame rate of about 10 ms for about 1000 × 1000 pixels in size, and some new findings on the olfactory processing were obtained. Such an improvement of the experimental apparatus will enable us to obtain further information not only on the olfactory processing of the land slug but also on various biological functions.



## Author details

Minoru Saito

Address all correspondence to: [msaito@chs.nihon-u.ac.jp](mailto:msaito@chs.nihon-u.ac.jp)

Department of Biosciences, College of Humanities and Sciences, Nihon University, Tokyo, Japan

## References

- [1] Molecular Probes TM Handbook; A Guide to Fluorescent Probes and Labeling Technologies. 11th ed. Invitrogen USA 2010
- [2] Orbach HS, Cohen LB, Grinvald A. Optical mapping electrical activity in rat somatosensory and visual cortex. *Journal of Neuroscience*. 1985;**5**(7):1886-1895
- [3] Kudo Y, Nakamura T, Ito E. A 'macro' image analysis of Fura-2 fluorescence to visualize the distribution of functional glutamate receptor subtypes in hippocampal slices. *Neuroscience Research*. 1991;**12**(3):412-420
- [4] Sato S, Osanai H, Monma T, Harada T, Hirano A, Saito M, Kawato S. Acute effect of corticosterone on *N*-methyl-D-aspartate receptor-mediated  $\text{Ca}^{2+}$  elevation in mouse hippocampal slices. *Biochemical and Biophysical Research Communications*. 2004;**321**(2):510-513
- [5] Ikegaya Y, Bon-Jero ML, Yuste R. Large-scale imaging of cortical network activity with calcium indicators. *Neuroscience Research*. 2005;**52**:132-138
- [6] Delaney KR, Gelperin A, Fee MS, Flores JA, Gervais R, Tank DW, Kleinfeld D. Waves and stimulus-modulated dynamics in an oscillating olfactory network. *Proceedings of the National Academy of Sciences of the United States of America*. 1994;**91**(2):669-673
- [7] Kleinfeld D, Delaney KR, Fee MS, Flores JA, Tank DW, Gelperin A. Dynamic of propagating waves in the olfactory network of a terrestrial mollusk: An electrical and optical study. *Journal of Neurophysiology*. 1994;**72**(3):1402-1419
- [8] Okada K, Kanzaki R, Kawachi K. High-speed voltage-sensitive dye imaging of an *in vivo* insect brain. *Neuroscience Letters*. 1996;**209**(3):197-200
- [9] Kawahara S, Toda S, Suzuki Y, Watanabe S, Kirino Y. Comparative study of neural oscillation in the procerebrum of the terrestrial slugs *Incilaria bilineata* and *Limax marginatus*. *Journal of Experimental Biology*. 1997;**200**(13):1851-1861
- [10] Kimura T, Toda S, Sekiguchi T, Kawahara S, Kirino Y. Optical recording analysis of olfactory response of the procerebral lobe in the slug brain. *Learning & Memory*. 1998;**4**:389-400

- [11] Inoue T, Kawahara S, Toda S, Watanabe S, Kirino Y. Selective optical recording of the neural activity in the olfactory center of the land slug using a calcium indicator dye. *Bioimages*. 1998;**6**(2):59-67
- [12] Yoshida R, Iwamoto A, Nagahama T. Calcium imaging for detection and estimation of spike activities in *Aplysia* neurons. *Zoological Science*. 2001;**18**(5):631-643
- [13] Watanabe S, Shimozone S, Kirino Y. Optical recording of oscillatory neural activities in the molluscan brain. *Neuroscience Letters*. 2004;**359**(3):147-150
- [14] Watanabe S, Kirino Y. Selective calcium imaging of olfactory interneurons in a land mollusk. *Neuroscience Letters*. 2007;**417**(3):246-249
- [15] Hamasaki Y, Hosoi M, Nakada S, Shimokawa T, Saito M. Fluorescent voltage imaging technique for measurement of molluscan neural activities. *Open Journal of Biophysics*. 2013;**3**:54-58
- [16] Hamasaki Y, Shimokawa T, Ishida K, Komatsuzaki Y, Watanabe S, Saito M. Coherency evaluation of spatiotemporal neural activities in the molluscan olfactory center applying extracellular recording with wavelet analysis. *Open Journal of Biophysics*. 2013;**3**:291-297
- [17] Ito I, Nakamura H, Kimura T, Suzuki H, Kirino Y, Ito E. Neuronal components of the superior and inferior tentacles in the terrestrial slug, *Limax marginatus*. *Neuroscience Research*. 2000;**37**(3):191-200
- [18] Ito I, Watanabe S, Kimura T, Kirino Y, Ito E. Distribution of  $\gamma$ -aminobutyric acid immunoreactive and acetylcholinesterase-containing cells in the primary olfactory system in the terrestrial slug *Limax marginatus*. *Zoological Science*. 2003;**20**(11):1337-1346
- [19] Ito I, Watanabe S, Kirino Y. Air movement evokes electro-olfactogram oscillations in the olfactory epithelium and modulates olfactory processing in a slug. *Journal of Neurophysiology*. 2006;**96**(4):1939-1948
- [20] Inokuma Y, Inoue T, Watanabe S, Kirino Y. Two types of network oscillations and their odor responses in the primary olfactory center of a terrestrial mollusc. *Journal of Neurophysiology*. 2002;**87**(6):3160-3164
- [21] Ito I, Watanabe S, Kimura T, Kirino Y, Ito E. Negative relationship between odor-induced spike activity and spontaneous oscillations in the primary olfactory system of the terrestrial slug *Limax marginatus*. *Zoological Science*. 2003;**20**(11):1327-1335
- [22] Ito I, Kimura T, Watanabe S, Kirino Y, Ito E. Modulation of two oscillatory networks in the peripheral olfactory system by  $\gamma$ -aminobutyric acid, glutamate, and acetylcholine in the terrestrial slug *Limax marginatus*. *Journal of Neurobiology*. 2004;**59**(3):304-318
- [23] Ratté S, Chase R. Morphology of interneurons in the procerebrum of the snail *Helix aspersa*. *Journal of Comparative Neurology*. 1997;**384**(3):359-372
- [24] Ratté S, Chase R. Synapse distribution of olfactory interneurons in the procerebrum of the snail *Helix aspersa*. *Journal of Comparative Neurology*. 2000;**417**(3):366-384

- [25] Zaitseva OV. Projectional connections and a hypothetical scheme of structural organization of procerebrums of terrestrial molluscs. *Journal of Evolutionary Biochemistry and Physiology*. 2000;**36**(5):604-620
- [26] Gelperin A, Tank DW. Odor-modulated collective network oscillations of olfactory interneurons in a terrestrial mollusc. *Nature*. 1990;**345**(6274):437-440
- [27] Watanabe S, Kawahara S, Kirino Y. Morphological characterization of the bursting and nonbursting neurons in the olfactory centre of the terrestrial slug *Limax marginatus*. *Journal of Experimental Biology*. 1998;**201**(7):925-930
- [28] Inoue T, Watanabe S, Kawahara S, Kirino Y. Phase-dependent filtering of sensory information in the oscillatory olfactory center of a terrestrial mollusk. *Journal of Neurophysiology*. 2000;**84**(2):1112-1115
- [29] Loew LM, Cohen LB, Dix J, Fluhler EN, Montana V, Salama G, Jian-young W. A naphthyl analog of the aminostyryl pyridinium class of potentiometric membrane dyes shows consistent sensitivity in a variety of tissue, cell, and model membrane preparations. *Journal of Membrane Biology*. 1992;**130**(1):1-10
- [30] Ermentrout GB, Wang JW, Flores J, Gelperin A. Model for olfactory discrimination and learning in *Limax* procerebrum incorporating oscillatory dynamics and wave propagation. *Journal of Neurophysiology*. 2001;**85**(4):1444-1452
- [31] Kimura T, Toda S, Sekiguchi T, Kirino Y. Behavioral modulation induced by food odor aversive conditioning and its influence on the olfactory responses of an oscillatory brain network in the slug *Limax marginatus*. *Learning & Memory*. 1998;**4**:365-375
- [32] Kimura T, Suzuki H, Kono E, Sekiguchi T. Mapping of interneurons that contribute to food aversive conditioning in the slug brain. *Learning & Memory*. 1998;**4**:376-388
- [33] Murakami M, Watanabe S, Inoue T, Kirino Y. Odor-evoked responses in the olfactory center neurons in the terrestrial slug. *Journal of Neurobiology*. 2004;**58**(3):369-378
- [34] Gelperin A. Nitric oxide mediates network oscillations of olfactory interneurons in a terrestrial mollusc. *Nature*. 1994;**369**(6475):61-63
- [35] Gelperin A, Flores J, Raccuia-Behling F, Cooke IRC. Nitric oxide and carbon monoxide modulate oscillations of olfactory interneurons in a terrestrial mollusc. *Journal of Neurophysiology*. 2000;**83**(1):116-127
- [36] Watanabe S, Takahashi F, Ishida K, Kobayashi S, Kitamura Y, Hamasaki Y, Saito M. Nitric oxide-mediated modulation of central network dynamics during olfactory perception. *PLoS One*. 2015;**10**(9):e0136846

